ELSEVIER

Journal of Organometallic Chemistry 492 (1995) 73–80

Journal of Organometallic Chemistry

Metal complexes of ferrocene cryptands

Herbert Plenio *, Ralph Diodone

Institut für Anorganische und Analytische Chemie, Univ. Freiburg, Albertstr. 21, 79104 Freiburg, Germany

Received 14 September 1994; revised 18 October 1994

Abstract

The reaction of 1,1'-ferrocenediyl(bismethylene-bispyridinium)-chloride-tosylate with diaza-15-crown-5 exclusively yields the 2 + 2-addition product 1,1'' : 1',1'''-bisferrocenediyl-bis[bis-7,13-methylene(1,4,10-trioxa-7,13-diazacyclopentadecane)] [=Fcdiyl(N_2-15-C-5)$_2$Fcdiyl]. The large cavities formed by Fcdiyl(N_2-15-C-5)$_2$Fcdiyl and Fcdiyl(N_2-18-C-6)$_2$Fcdiyl can accommodate two metal ions simultaneously, resulting in large iron–cation distances. The X-ray crystal structures of Fcdiyl(N_2-15-C-5)$_2$Fcdiyl · 2Na(p-tosylate), Fcdiyl(N_2-18-C-6)$_2$Fcdiyl · $(RbI)_2$, 1,1'-ferrocenediyl[bis-7,16-methylene(1,4,10,13-tetraoxa-7,16-diazacyclooctadecane)] · $Ca(ClO_4)_2$ [=Fcdiyl(N_2-18-C-6) · $Ca(ClO_4)_2$] and Fcdiyl(N_2-18-C-6) · $Ba(ClO_4)_2$ were determined to gain a better understanding of the metal complexation in ferrocene cryptands and to explore the possibility of direct iron–cation interactions. Fcdiyl(N_2-18-C-6) · $Ca(ClO_4)_2$ displays an unusually short Fe–Ca^{2+} distance (365.8(6) pm) which might be viewed as an Fe–Ca^{2+} interaction. The ammonium salts formed upon protonation of Fcdiyl(N_2-15-C-5)$_2$Fcdiyl and Fcdiyl(N_2-18-C-6)$_2$Fcdiyl can be oxidized reversibly but the addition of anions gave no significant cathodic shifts of the redox potentials.

Keywords: Ferrocene; Cryptands; X-ray structure; Group 1; Group 2

1. Introduction

Ferrocene crown ethers and ferrocene cryptands both provide a redox active site as well as a cation binding unit [1]. Upon oxidation of the ferrocene subcomponent the stability of the macrocycle–cation complex is reduced (redox-switched crown ethers) [2] owing to the proximity of the positively charged ferrocene group to the crown ether bound cation [3,4]. We recently described a high yield synthesis of 1,1'-ferrocenediyl-[bis-7,16-methylene(1,4,10,13-tetraoxa-7,16-diazacyclooctadecane)] (**4**) and 1,1'' : 1',1'''-bisferrocenediyl-bis[bis-7,16-methylene(1,4,10,13-tetraoxa-7,16-diazacyclooctadecane)] (**3**) and demonstrated the redox-switched bonding of metal ions and protons [5]. The ferrocene-clamped 18-membered macrocycle holds cations very close to the redox-active center thereby producing large shifts in the redox potential upon coordination of metal salts [6]. We were interested therefore whether 1,1'-ferrocenediyl(bismethylene-bispyridinium)chloride-tosylate (**1**) could also be used for the synthesis of ferrocene cryptands with smaller cavities. Such compounds would hold metal ions even closer to the iron atom and the smaller cavities could selectively coordinate small, highly charged metal ions. This should result in much larger redox responses upon complexation of metal ions and the possibility of iron–cation interactions.

2. Results and discussion

The reaction of 1,1'-ferrocenediyl(bismethylene-bispyridinium)chloride-tosylate (**1**) with 1,4,10-trioxa-7,13-diazacyclopentadecane (N_2-15-C-5) and Na_2CO_3 in acetonitrile under reflux yielded 1,1'' : 1',1'''-bisferrocenediyl-bis[bis-7,13-methylene(1,4,10-trioxa-7,13-diazacyclopentadecane)] (**2**) (Scheme 1). After chromatographic purification, **2** was obtained as its complex with two molecules of Na(*p*-tosylate). The complex formed by Na^+, the lipophilic tosylate anion and the crown ether **2** is too stable to dissociate during chromatography. Pure **2** is isolated only when a $CHCl_3$ solution of sodium complex is extracted with water, either before or after chromatography.

The exclusive formation of the 2 + 2 product is

* Corresponding author.

SSDI 0022-328X(94)05272-7

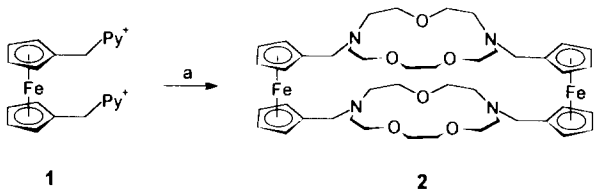

Scheme 1. Synthesis of the ferrocene cryptand **2**; a + diaza-15-crown-5, Na_2CO_3.

surprising since in the corresponding reaction of diaza-18-C-6 the 1 + 1 product **4** is mainly formed, together with smaller amounts of 2 + 2 product **3** [5]. Our initial idea was that Na^+ used in the condensation reaction was the wrong templating metal ion. However, attempts to modify reaction conditions such as using other metal ion templates, non-templating bases or different concentrations of the reactands never resulted in the formation of the desired 1 + 1 product.

It was obvious that only small redox-switching effects could be expected from **2** since the distance of metal ions bound within the 15-membered macrocycle from the redox-active center is quite large (see Section

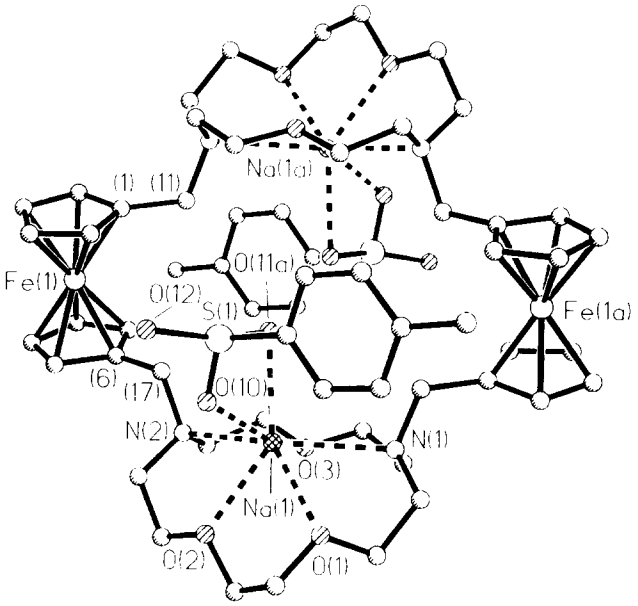

Fig. 1. Molecular structure of **2**·2 Na(*p*-tosylate) (without hydrogen atoms). Carbon atoms are denoted by numbers only. Selected interatomic distances are as follows: Fe(1)–Fe(1a), 1094 pm; Fe(1)–Na(1), 642.3 pm; Na(1)–Na(1a), 701.9 pm.

Table 1
Crystal data summary

Identification code	2 · 2Na(*p*-tosylate)	3 · $(RbI)_2$	4 · $Ca(ClO_4)_2 \cdot H_2O$	4 · $Ba(ClO_4)_2 \cdot H_2O$
Empirical formula	$C_{58}H_{78}Fe_2N_4Na_2O_{12}S_2$	$C_{50}H_{74}Cl_6Fe_2I_2N_4O_8Rb_2$	$C_{24}H_{38}CaCl_2FeN_2O_{13}$	$C_{24}H_{38}BaCl_2FeN_2O_{13}$
Formula weight	1245.1	1608.3	729.40	826.71
Temperature (K)	293(2)	293(2)	213(2)	293(2)
Wavelength (pm)	71.069	71.069	71.069	71.069
Crystal system	Monoclinic	Monoclinic	Monoclinic	Triclinic
Space group	$P2_1/c$	$P2_1/n$	$C2/c$	$P\text{-}1$
Unit cell				
a (pm)	1402.2(3)	1407.8(3)	1563.7(3)	1036.8(2)
b (pm)	1032.2(2)	1856.2(4)	1213.8(2)	1112.7(2)
c (pm)	2051.4(4)	1427.4(3)	1625.3(3)	1509.0(3)
α (°)	90	90	90	102.43(3)
β (°)	92.10(3)	93.89(3)	98.06(3)	97.38(3)
γ (°)	90	90	90	94.23(3)
Volume (Å^3)	2967.1(10)	3721.4(14)	3054.4(10)	1676.7(6)
Z	2	2	2	2
Density (g cm^{-3})	1.392	1.435	1.586	1.835
Absorption (mm^{-1})	0.920	2.78	0.768	1.84
$F(000)$	1312	1600	808	876
θ range [°]	2.5–26.3	2.2–22.3	3.6–25.0	2.6–26.3
Index range (h, k, l)	−17–16, −12–0, −24–0	0–15, 0–19, −15–14	0–18, 0–14, −19–19	−12–12, 0–13, −18–18
Number of reflections				
Collected	5362	4827	2802	7164
Independent	5207	4384	2185	6801
Number of data; number of parameters	4034; 378	3456; 374	2060; 223	6411; 416
Goodness of fit	1.068	1.012	1.058	1.131
R index ($2\sigma(I)$)				
R_1	8.99	8.37	6.67	3.92
wR_2	25.13	24.09	18.71	10.23
Largest peak	+0.60	+1.43	+0.66	+1.30
Largest hole (electrons Å^{-3})	−1.89	−1.18	−0.49	−0.44

3). The ferrocene cryptand **2** displays only one reversible redox couple at $E_{1/2} = +0.39$ V which corresponds to the simultaneous oxidation of both ferrocene groups. The addition of metal salts to a solution of **2** in CH_3CN gives anodic shifts (Li^+, $E_{1/2} = +0.435$ V and $\Delta = +45$ mV; Na^+, $E_{1/2} = +0.47$ V and $\Delta = +80$ mV); again only one reversible wave for the two ferrocene units is observed.

Since the 2 + 2 products of the reactions of diaza-18-C-6 and diaza-15-C-5 with **1** possess huge cavities between the two ferrocene units and the two crown ether rings we were intrigued to explore, whether it was possible to coordinate anions within this void [7].

Table 2
Atomic coordinates and equivalent isotropic displacement parameters for **2**·2Na(p-tosylate), where U_{eq} is defined as one third of the trace of the orthogonalized U_{ij} tensor

	x ($\times 10^{-4}$)	y ($\times 10^{-4}$)	z ($\times 10^{-4}$)	U_{eq} ($\times 10^{-3}$ Å^2)
Fe(1)	1896(1)	629(1)	1509(1)	38(1)
Na(1)	6451(2)	48(3)	1431(2)	44(1)
C(1)	1943(5)	1230(8)	565(4)	40(2)
C(2)	996(6)	1026(9)	739(4)	47(2)
C(3)	789(7)	1820(10)	1260(4)	54(2)
C(4)	1616(8)	2548(9)	1423(5)	60(3)
C(5)	2331(7)	2204(8)	992(4)	49(2)
C(6)	3108(5)	−207(8)	1870(4)	39(2)
C(7)	2505(6)	−1159(9)	1574(5)	50(2)
C(8)	1633(6)	−1155(10)	1912(6)	63(3)
C(9)	1698(7)	−202(11)	2399(5)	63(3)
C(10)	2605(6)	370(9)	2382(4)	51(2)
C(11)	2486(5)	612(9)	29(4)	44(2)
N(1)	2289(4)	1114(7)	−640(3)	43(2)
C(12)	1309(5)	813(10)	−864(4)	55(2)
C(13)	1205(6)	727(10)	−1604(5)	61(3)
O(1)	1768(4)	−342(7)	−1814(3)	56(2)
C(14)	1698(7)	−576(12)	−2494(5)	65(3)
C(15)	2393(6)	177(11)	−2869(4)	54(2)
O(2)	3310(4)	−141(7)	−2627(3)	53(2)
C(16)	2489(6)	2501(9)	−695(4)	49(2)
C(17)	4109(5)	127(8)	1649(4)	42(2)
N(2)	4892(4)	−550(7)	2018(3)	41(2)
C(18)	4809(6)	−1958(8)	1989(4)	45(2)
C(19)	5082(5)	−2506(9)	1338(4)	49(2)
O(3)	6102(4)	−2223(6)	1278(3)	44(1)
C(20)	6469(6)	−2816(9)	713(4)	51(2)
C(21)	5021(6)	−66(10)	2677(4)	52(2)
C(22)	5954(6)	−366(11)	3001(5)	60(3)
S(1)	5693(2)	2876(5)	943(2)	201(2)
O(10)	6024(5)	2311(7)	1518(3)	64(2)
O(11A)	5607(11)	1326(13)	566(7)	73(4)
O(12)	5384(9)	4457(13)	1327(6)	57(3)
C(50)	6667(7)	3302(9)	475(5)	56(3)
C(51)	6548(9)	4018(10)	−84(5)	70(3)
C(52)	7309(12)	4315(11)	−453(5)	80(4)
C(53)	8229(11)	3925(11)	−287(5)	77(3)
C(54)	8354(9)	3179(10)	280(5)	71(3)
C(55)	7570(9)	2896(10)	653(5)	66(3)
C(56)	9051(12)	4248(15)	−692(6)	109(5)

Symmetry operation used to generate equivalent atoms, $1-x$, $-y$, $-z$.

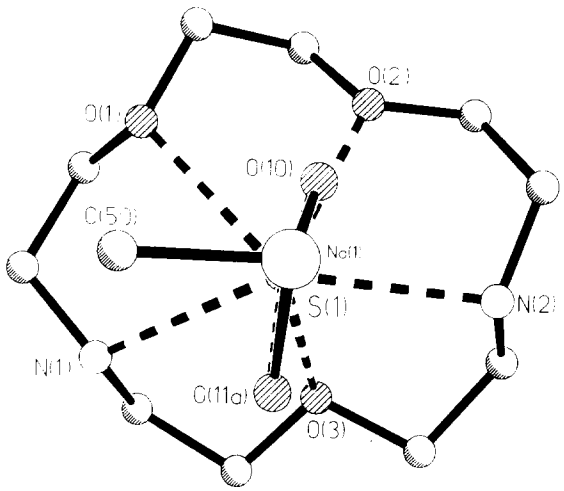

Fig. 2. Coordination sphere of Na^+ in **2**·2Na(*p*-tosylate), viewed along the Na–S vector. Selected bond lengths and angles are as follows: Na–O(1), 260.9(6) pm; Na–O(2), 246.6(6) pm; Na–O(3), 241.2(7) pm; Na–N(1), 272.2(7) pm; Na–N(2), 260.7(7) pm; Na–O(10), 242.0(8) pm; Na–O(11a), 248(2) pm; S(1)–O(10), 137.9(6) pm; S(1)–O(11a), 177.9(13) pm; N(1)–Na(1)–N(2), 138.1(3)°. O(11a) and O(20b) were refined with a site occupancy factor of $\frac{1}{2}$. O(3) and O(11a) are located inside with respect to the center of the whole molecule. C(50) is the pivot atom of the tolyl unit. Only one component of the disordered SO_3 group is displayed.

Since protonated macrocyclic polyamines have been used for the complexation of anions [8,9], our ferrocene cryptands had to be modified by treating them with acid to generate protonated polyamines.

To avoid potentially hazardous perchlorates we had initially chosen CF_3SO_3H for protonation. Unfortunately, however, only yellow oils could be isolated, which resisted all attempts to crystallize. On the contrary treatment of the ferrocene cryptands **2** and **3** with $HClO_4$ gives beautiful crystalline ammonium salts, which can be purified easily by recrystallization from CH_3CN–Et_2O. The protonated ferrocene cryptands are oxidized reversibly at potentials shifted anodically by more than 300 mV with respect to the neutral ferrocene macrocycles (**2** · $4HClO_4$, $E_{1/2} = +0.73$ V; **3** · $4HClO_4$, $E_{1/2} = +0.71$ V). However, upon addition of Cl^-, NO_3^-, HSO_4^- or SO_4^{2-} to solutions of **2** · $4HClO_4$ or **3** · $4HClO_4$ in $CH_3CN \cdot H_2O$ (80:20) no shifts of the redox potentials larger than 25 mV were observed.

3. Discussion of the X-ray crystal structures

To obtain an idea of the approximate size of the cavities of the 2 + 2 addition products we determined the solid state structures of the metal complexes **2** · 2 Na(*p*-tosylate) and **3** · $(RbI)_2$.

In the solid state structure of **2** · 2 Na(*p*-tosylate) each of the two 15-membered crown ether rings coordinates one Na(*p*-tosylate) (Fig. 1 and Table 2). This

rather independent behaviour of the two macrocycles has also been observed for other cyclindrical macrocycles [10]. The torsion angle C(11)–C(1)–C(6)–C(17), which determines the distance of the two crown ether units, is 50.4°. The bonding of Na^+ sitting above the 15-membered macrocycle is not symmetrical with respect to the donor atoms and the metal ion is displaced towards N(2) (Fig. 2). Therefore there are shorter (N(2), O(2) and O(3)) and longer (N(1) and O(1)) bonds to Na^+. Not unexpectedly the small size of Na^+ does not allow a sandwiching of this cation between the two 15-membered macrocycles. However, the five-fold coordination provided by the five donor atoms in the diaza-15-crown-5 unit does not saturate the coordination sphere of Na^+. The tosylate group therefore provides one or two additional oxygen donors, depending on the orientation of the disordered SO_3 group. The tosylate group acts either as a chelating bidentate or as a monodentate ligand. In the latter case, one water molecule (Na–O(20b), 261.1(13) pm) occupies the seventh coordination site at sodium, but further inside the cavity than O(11a). In both cases, O(10), which has a sulfur–oxygen double bond (S(1)–O(10), 138.3(6) pm), remains bonded to Na^+. Somewhat surprisingly the two Na(*p*-tosylate) units are located on the inside of the cavity and not on the outside, as might have been expected on the basis of steric arguments. However, a closer look reveals that this endohedral coordination is enforced, because it allows the best interaction of the nitrogen lone pairs with Na^+ and minimizes steric contacts between the two crown ether rings.

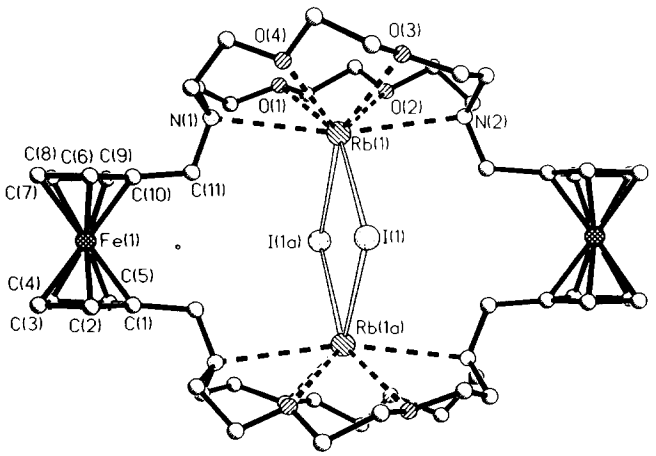

Fig. 3. Molecular structure of $3 \cdot (RbI)_2$ in the crystal (without hydrogen atoms). Selected bond lengths, angles and interatomic distances are as follows: Rb(1)–I(1), 361.6(2) and 366.5(2) pm; Rb(1)–O(2), 293.5(10) pm; Rb(1)–O(4), 296.1(11) pm; Rb(1)–O(1), 298.9(10) pm; Rb(1)–O(3), 302.0(11) pm; Rb(1)–N(2), 319.7(12) pm; Rb(1)–N(1), 318.2(13) pm, Fe(1)–Fe(1a) 1274 pm; Rb(1)–Rb(1a), 545.9 pm; N(1)–Rb(1)–N(2), 165.4(3) pm; C(9)–C(10)–C(11)–N(1), 87.6°.

Table 3
Selected atomic coordinates and equivalent isotropic displacement parameters for $3 \cdot (RbI)_2$, where U_{eq} is defined as one third of the trace of the orthogonalized U_{ij} tensor

	x ($\times 10^{-4}$)	y ($\times 10^{-4}$)	z ($\times 10^{-4}$)	U_{eq} ($\times 10^{-2}$ Å^2)
I(1)	455(1)	1121(1)	4309(1)	78(1)
Rb(1)	−1161(1)	745(1)	6108(1)	47(1)
Fe(1)	3002(1)	−409(1)	8503(2)	54(1)
C(1)	3163(11)	−780(9)	7189(11)	59(4)
C(2)	3911(9)	−316(9)	7459(10)	57(4)
C(3)	4386(11)	−621(12)	8336(12)	75(6)
C(4)	3934(13)	−1236(11)	8518(13)	75(5)
C(5)	3145(12)	−1376(10)	7823(11)	68(5)
C(6)	2524(10)	583(9)	8784(12)	62(4)
C(7)	2978(13)	281(10)	9633(12)	70(5)
C(8)	2536(11)	−345(10)	9822(11)	62(4)
C(9)	1768(11)	−441(9)	9136(11)	57(4)
C(10)	1753(10)	129(8)	8508(10)	53(4)
C(11)	1001(9)	269(8)	7722(10)	48(4)
N(1)	216(7)	746(6)	7972(8)	51(3)
C(12)	−291(10)	453(10)	8735(10)	63(4)
C(13)	−928(11)	−180(11)	8452(11)	73(5)
O(1)	−1741(6)	77(5)	7894(6)	51(2)
C(14)	−2402(12)	−485(9)	7666(11)	66(5)
C(15)	−3310(11)	−126(10)	7180(12)	70(5)
O(2)	−3056(6)	120(6)	6298(7)	61(3)
C(16)	−3837(11)	476(10)	5823(11)	67(5)
C(17)	−3683(10)	502(9)	4804(10)	58(4)
N(2)	−2895(7)	976(6)	4571(8)	48(3)
C(18)	−3151(11)	1728(8)	4535(12)	64(4)
C(19)	−2363(14)	2240(8)	4696(12)	76(5)
O(3)	−1980(7)	2215(5)	5632(7)	62(3)
C(20)	−1293(13)	2730(8)	5848(14)	77(5)
C(21)	−1062(12)	2719(7)	6881(12)	64(4)
O(4)	−532(8)	2089(6)	7085(8)	70(3)
C(22)	−210(12)	2047(9)	8046(12)	75(5)
C(23)	531(11)	1479(9)	8197(12)	70(5)
C(24)	−2496(9)	742(7)	3696(10)	46(4)

Symmetry operation used to generate equivalent atoms, $-x$, $-y$, $1-z$.

The same rules are followed in the structure of $3 \cdot (RbI)_2$ (Fig. 3 and Table 3). The 2 + 2 addition product of the pyridinium salt **1** and diaza-18-C-6 is characterized by an even larger cavity. In the solid state structure of $3 \cdot (RbI)_2$, two RbI units are sandwiched between the two 18-membered macrocycles, which is somewhat similar to the complex formed by 18-C-6 and RbNCS [11]. The interiron distance of 1274 pm is shorter than the 1457 pm found in the structure of the tetraamido analogue of **4** [12]. To accommodate four such large atoms (two RbI) the torsion angle C(6)–C(9)–C(11)–N(1) of 82.3° is close to the maximum value of 90° and there are no unfavorable van der Waals interactions (Fig. 4). The Rb–I (364 pm), Rb–Rb (546 pm) and the I–I (482 pm) distances may be compared with the respective values observed in the solid-state structure of RbI (Rb–I, 367 pm; Rb–Rb and I–I, 519 pm) [13].

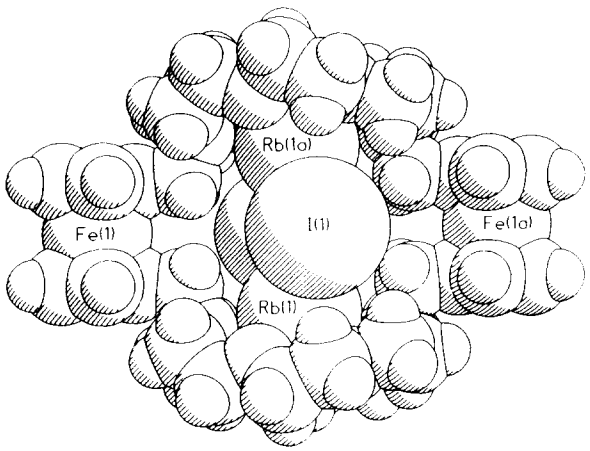

Fig. 4.

In contrast with the 2 + 2 products (**2**, **3**), the corresponding monomer **4** is characterized by a much smaller cavity, resulting in short Fe–cation distances. A comparison of the structures of **4** · $Ca(ClO_4)_2$ (Fig. 5 and Table 4) and **4** · $Ba(ClO_4)_2$ (Fig. 6 and Table 5) shows that Ca^{2+} sits inside the cavity, whereas Ba^{2+} is too large and is located above the macrocycle. Consequently both perchlorate groups and one water molecule are bound to Ba^{2+} (Coordination number (CN), 9), whereas one water molecule is sufficient for the coordination sphere of Ca^{2+} (CN, 7) (both perchlorate groups are linked to this water molecule via bridging hydrogen atoms). Whereas Ca^{2+} ideally fits into the cavity of the ferrocene cryptand, the opposite is the case for Ba^{2+}, which does not coordinate at all to N(1) and also has a rather long Ba(1)–O(4) bond of 304.6(3) pm. In **4** · $Ca(ClO_4)_2$ the two vectors C(5)–C(6) and C(5a)–C(6a) form an angle of 103°, whereas the analogous angle in **4** · $Ba(ClO_4)_2$ is only 44.7°. In the case of **4** · $Ca(ClO_4)_2$ this leads to an opening up of the crown ether ring and an efficient encapsulation of the metal ion. The Ca^{2+}–O bonds (average, 244 pm) are somewhat shorter than usual (251 pm) [14,15] and in the [2.2.2]-cryptand (249–255 pm) [16,17].

It is very interesting to compare the structure of **4** · $Ca(ClO_4)_2$ with **4** · $NaClO_4$ and **4** · $AgClO_4$ which both were described by Gokel and coworkers [3].

Table 4
Selected atomic coordinates and equivalent isotropic displacement parameters for **4** · $Ca(ClO_4)_2 \cdot H_2O$ where U_{eq} is defined as one third of the trace of the orthogonalized U_{ij}b tensor

	x ($\times 10^{-4}$)	y ($\times 10^{-4}$)	z ($\times 10^{-4}$)	U_{eq} ($\times 10^{-3}$ Å^2)
Fe(1)	5000	1122(1)	2500	27(1)
C(1)	4654(3)	282(3)	3510(3)	32(1)
C(2)	4115(3)	1206(4)	3307(3)	38(1)
C(3)	4642(3)	2160(4)	3370(3)	42(1)
C(4)	5505(3)	1829(3)	3602(3)	37(1)
C(5)	5522(3)	653(4)	3687(2)	31(1)
C(6)	6309(3)	8(4)	3988(3)	43(1)
N(1)	6381(2)	−1080(3)	3564(3)	39(1)
C(7)	7123(3)	−1030(5)	3090(4)	50(1)
C(8)	7194(3)	−2020(5)	2551(4)	59(2)
C(9)	6532(4)	−1977(4)	4205(3)	48(1)
C(10)	5738(4)	−2183(4)	4601(3)	50(1)
O(1)	5056(2)	−2484(3)	3962(2)	45(1)
C(11)	4281(4)	−2718(5)	4313(4)	59(2)
C(12)	3581(4)	−2995(5)	3605(4)	59(2)
O(2)	3602(2)	−2141(3)	2994(2)	49(1)
Ca(1)	5000	−1891(1)	2500	32(1)
O(21)	5000	−3858(4)	2500	55(2)

Symmetry operations used to generate equivalent atoms, $1-x$, y, $0.5-z$.

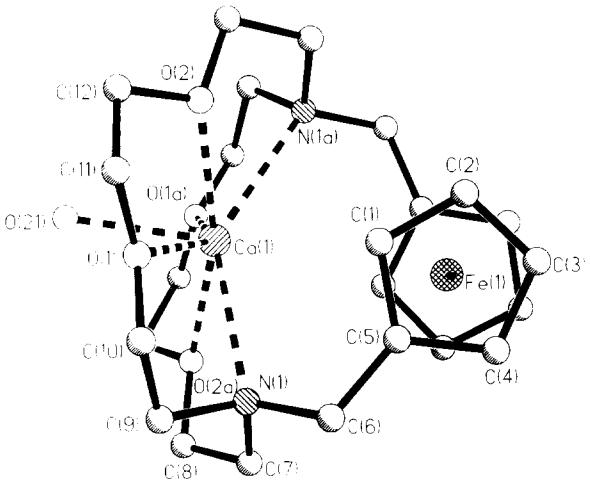

Fig. 5. Molecular structure of **4**·$Ca(ClO_4)\cdot H_2O$ in the crystal (without hydrogen atoms). Selected bond lengths and angles are as follows: Ca(1)–O(21), 238.7(4) pm; Ca(1)–O(1) 247.2(3) pm; Ca(1)–O(2), 245.2(3) pm; Ca(1)–N(1), 275.2(4) pm; Ca(1)–Fe(1), 365.8(6) pm; N(1)–Ca(1)–N(1a), 138.1(2)°; Cp–Cp′, 11.0 pm; C(6)–C(5)–C(5a)–C(6a), 103.0°.

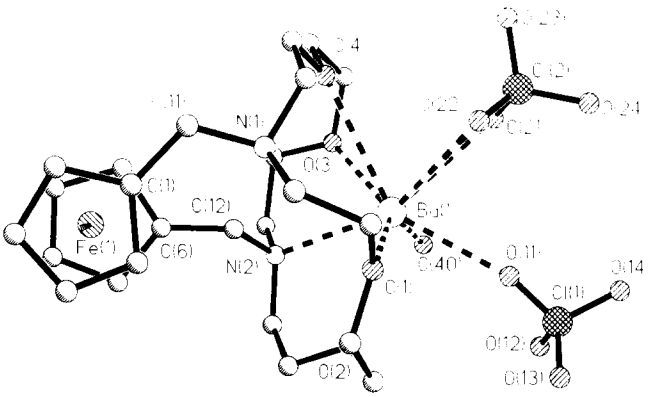

Fig. 6. Molecular structure of **4**·$Ba(ClO_4)_2\cdot H_2O$ in the crystal (without hydrogen atoms). Selected bond lengths, interatomic distances and angles are as follows: Ba(1)–O(1), 280.0(3) pm; Ba(1)–O(2), 282.4(3) pm; Ba(1)–O(3), 276.8(3) pm; Ba(1)–O(4), 304.6(3) pm; Ba(1)–O(40), 270.2(3) pm; Ba(1)–O(11), 270.0(4) pm, Ba(1)–O(21), 289.7 (3) pm; Ba(1)–O(22), 296.2(3) pm; Ba(1)–N(2), 286.8(3) pm; Ba(1)–Fe(1), 609.0 pm; Ba(1)–N(1), 398.8 pm; Cp–Cp; 2.6 pm; C(11)–C(1)–C(6)–C(12) 44.7°. O(2) lies behind the carbon atom.

Table 5
Selected atomic coordinates and equivalent isotropic displacement parameters for $4 \cdot Ba(ClO_4)_2 \cdot H_2O$, where U_{eq} is defined as one third of the trace of the orthogonalized U_{ij} tensor

	x ($\times 10^{-4}$)	y ($\times 10^{-4}$)	z ($\times 10^{-4}$)	U_{eq} ($\times 10^{-3}$ Å^2)
Ba(1)	1670(1)	596(1)	3315(1)	39(1)
Fe(1)	5693(1)	3716(1)	1925(1)	44(1)
C(1)	4560(4)	2563(4)	782(3)	51(1)
C(2)	5543(4)	1920(4)	1159(3)	56(1)
C(3)	6756(5)	2551(5)	1158(4)	75(2)
C(4)	6575(6)	3578(6)	788(4)	92(2)
C(5)	5211(6)	3589(5)	553(3)	80(2)
C(6)	4943(3)	3705(3)	3108(2)	41(1)
C(7)	4570(4)	4739(4)	2753(3)	57(1)
C(8)	5737(5)	5467(4)	2699(4)	65(1)
C(9)	6813(4)	4903(4)	3028(3)	57(1)
C(10)	6341(4)	3812(4)	3272(3)	50(1)
C(11)	3103(4)	2243(4)	527(3)	54(1)
C(12)	4003(3)	2645(3)	3174(2)	40(1)
N(1)	2470(3)	1330(3)	959(2)	42(1)
C(13)	2741(4)	81(4)	511(2)	49(1)
C(14)	2289(4)	−927(4)	962(2)	51(1)
O(1)	2835(3)	−772(3)	1905(2)	49(1)
C(15)	4112(4)	−1161(4)	2047(3)	54(1)
C(16)	4395(4)	−1259(4)	3030(3)	52(1)
O(2)	4202(2)	−139(2)	3656(2)	48(1)
C(17)	5340(4)	732(4)	3924(3)	53(1)
C(18)	4992(4)	1889(4)	4506(3)	51(1)
N(2)	3864(3)	2408(3)	4087(2)	39(1)
C(19)	3540(4)	3467(4)	4754(3)	49(1)
C(20)	2309(4)	3985(3)	4419(3)	52(1)
O(3)	1285(3)	2993(2)	4134(2)	46(1)
C(21)	154(4)	3515(4)	2788(3)	55(1)
C(22)	85(4)	3345(4)	3732(3)	56(1)
O(4)	549(3)	2417(2)	2255(2)	49(1)
C(23)	579(4)	2525(4)	1341(3)	59(1)
C(24)	1043(4)	1404(4)	780(3)	53(1)
O(40)	1616(4)	966(4)	5139(2)	79(1)
Cl(1)	1180(1)	−2670(1)	3979(1)	54(1)
O(11)	1144(5)	−1746(5)	3492(5)	133(2)
O(12)	1707(6)	−2199(9)	4894(4)	177(3)
O(13)	2016(6)	−3497(4)	3575(5)	138(2)
O(14)	−80(4)	−3259(4)	3918(3)	94(1)
Cl(2)	−1660(1)	−440(1)	2422(1)	52(1)
O(21)	−1117(3)	213(3)	3344(2)	60(1)
O(22)	−580(3)	−602(3)	1908(2)	61(1)
O(23)	−2553(4)	262(6)	2035(3)	120(2)
O(24)	−2296(4)	−1594(4)	2446(3)	101(1)

Whereas Na^+ and Ca^{2+} have almost identical ionic radii (Na^+_{VI}, 102 pm; Ca^{2+}_{VI}, 100 pm) [18], the two solid state structures are quite different. In $4 \cdot NaClO_4$ the Na^+–Fe distance is 439 pm whereas in $4 \cdot Ca(ClO_4)_2$ the distance Ca^{2+}–Fe, equals 365.8 pm, and is 73 pm shorter but still about 29 pm longer than in the Ag^+ complex. It was suggested that the short Ag–Fe distance and the 10° tilt of the two cyclopentadienyl rings are indicative of significant Ag → Fe interactions [3], which have been postulated for other ferrocene–metal complexes as well [19]. In $4 \cdot Ca(ClO_4)_2$ the opening up of the cyclopentadienyl rings to accommodate the approaching Ca^{2+} is even more pronounced (11.0°). This may or may not be viewed as an indication for an Fe → Ca^{2+} interaction; however, the UV spectra of the Ca^{2+} and the Na^+ complex are virtually identical, whereas that of the Ag^+ complex displays a red shift.

In conclusion it can be said that the dimeric ferrocene cryptands **2** and **3** possess extremely large cavities which can accommodate correspondingly large metal salts. The ferrocene cryptand **4** is best suited to the complexation of metal ions intermediate in size between Ca^{2+} and Ag^+ (ionic radii, 100–115 pm), whereas Ba^{2+} clearly is too large. Even so $4 \cdot Ca(ClO_4)_2$ displays some of the features (short distance Ca^{2+}–Fe; Cp–Cp′ tilt) indicative of a metal–metal interaction; evidence for a stabilizing Fe → Ca^{2+} interaction is not conclusive and remains a target for future investigations.

4. Experimental details

Commercially available solvents and reagents were purified according to literature procedures. Chromatography was carried out with silica MN 60. NMR spectra were recorded at 300 K with a Bruker AC200 F (^{1}H NMR, 200 MHz; ^{13}C NMR, 50 MHz) or a Varian Unity 300 (^{1}H NMR, 300 MHz; ^{13}C NMR, 75 MHz). ^{1}H NMR signals were referenced to residual hydrogen impurities in the solvent and ^{13}C NMR to the solvent signals: $CDCl_3$ (7.26 and 77.0 ppm), CD_3CN (1.93 and 1.30 ppm), dimethylsulfoxide d_6 (DMSO-d_6) (2.49 ppm). Elemental analyses were performed at the Mikroanalytisches Laboratorium der Chemischen Laboratorien, Universität Freiburg. Melting points were determined with a Meltemp melting-point apparatus in sealed capillaries. Starting materials were commercially available or prepared according to literature procedures: 1,1′-ferrocenediyl[bismethylene-bispyridinium] chloride-tosylate [20], 1,1″ : 1′,1‴-bisferrocenediyl-bis-[bis-7,16-methylene(7,16-diaza-1,4,10,13-tetraoxacyclooctadecane)] [5], 1,1′-ferrocenediyl[bis-7,16-methylene (1,4,10,13-tetraoxa-7,16-diazacyclooctadecane)] [5].

4.1. Cyclic voltammetry

The standard electrochemical instrumentation consisted of an Amel System 5000 potentiostat–galvanostat. Cyclic voltammograms were recorded using Amel software on a PC. A three-electrode configuration was employed. The working electrode was a Pt disk (diameter, 1 mm) sealed in soft glass. The counterelectrode was a Pt disk (area, 3 cm^2). The pseudoreference electrode was an Ag wire. Potentials were calibrated against the formal potential of cobaltocenium perchlorate (−0.94 V vs. Ag/AgCl). NBu_4PF_6 (0.1 M) was used as a supporting electrolyte.

Caution. Care has to be exercised when handling the solid perchlorate salts since they decompose violently at temperatures higher than 150°C.

4.2. 1,1'' : 1',1'''-Bisferrocenediyl-bis[bis-7,13-methylene(7,13-diaza-1,4,10-trioxacyclopentadecane)] (2)

0.5 g (2.35 mmol) of 7,13-diaza-1,4,10-trioxacyclopentadecane, 1.36 g (2.35 mmol) of 1,1'-ferrocenediyl[bismethylene-bispyridinium]-chloride-tosylate and 1.5 g or Na_2CO_3 in 100 ml on CH_3CN were heated under reflux for 16 h. The cold reaction mixture was filtered and the solvent evaporated. The oily residue was dissolved in 40 ml of CH_2Cl_2 and washed twice with 20 ml of water. The organic layer was separated and dried over $MgSO_4$ and then the solvent removed in vacuo. Chromatographic purification (silica; cyclohexane: diethylamine, 10:1) gave **2** as a yellow oil (yield, 0.35 g (35%)). When the raw material is not extracted with water, the product isolated after chromatography is (**2**) · 2Na(p-tosylate).

^{1}H NMR ($CDCl_3$): δ 2.61 (t, J = 4.9 Hz, 8H, NCH_2), 2.73 (t, J = 5.7 Hz, 8H, NCH_2), 3.48–3.63 (m, 32 H, OCH_2, $FcCH_2$), 4.04 (s, 16 H, FcH). ^{1}H NMR (CD_3CN): δ 2.54 (t, J = 5.1 Hz, 8H, NCH_2), 2.61 (t, J = 5.7 Hz, 8H, NCH_2), 3.43–3.55 (m, 32H, OCH_2, $FcCH_2$), 4.06, 4.07, 4.09, 4.10 (AA'BB', FcH). ^{13}C NMR ($CDCl_3$): δ 53.21 (NCH_2), 53.56 (NCH_2), 55.00 (OCH_2), 68.28 (OCH_2), 68.91 (OCH_2), 69.98 ($FcCH_2$), 70.44 (FcH), 70.68 (FcH), 83.18 (Fc). ^{13}C NMR (CD_3CN): δ 54.59 (NCH_2), 54.88 (NCH_2), 55.79 (OCH_2), 69.16 (OCH_2), 69.82 (OCH_2), 70.62 ($FcCH_2$), 71.14 (Fc), 71.66 (Fc), 85.14 (Fc). Mass spectrometry (electron impact, 70 eV): m/e 856 (M^+). Anal. Found: C, 61.13: H, 7.87: N, 6.22. $C_{44}H_{64}Fe_2N_4O_6$ (856.72) Calc.: C, 61.69; H, 7.53; N, 6.65.

4.3. (2) · 2NaBPh$_4$

^{1}H NMR (CD_3CN): δ 2.45–2.55 (m, 16H, NCH_2), 3.37 (t, J = 4.8 Hz, 8H, OCH_2), 3.49 (s, 16H, OCH_2), 3.55 (s, 8H, $FcCH_2$), 4.15, 4.16, 4.18, 4.19 (AA'BB', FcH). ^{13}C NMR (CD_3CN): δ 52.92 (NCH_2), 54.25 (NCH_2), 54.80 (OCH_2), 67.50 (OCH_2), 67.90 (OCH_2), 69.69, 70.39, 72.00, 83.11 (Fc).

4.4. (2) · 2Na(p-tosylate)

^{1}H NMR (DMSO-d_6): δ 2.29 (s, CH_3), 2.49 (s, NCH_2, br), 3.48–3.64 (m, OCH_2, $FcCH_2$), 4.15 (s, br, FcH), 7.11 ("d", J = 3.8 Hz, ArH), 7.50 ("d", J = 4.0 Hz, ArH).

4.5. (2) · 4HClO$_4$

To a stirred solution of **2** (100 mg,) in 10 ml of acetonitrile and 10 ml of water was added dilute $HClO_4$ up to pH < 3. The volume of the solution was reduced to one third in vacuo and the product was precipitated by addition of 10 ml of concentrated aqueous $LiClO_4$. The precipitate was filtered off and washed several times with small amounts of ice-cooled water. The yellow product was dried in vacuo for 6 h and recrystallized from CH_3CN–Et_2O (yield, 74 mg (53%)).

^{13}C NMR (CD_3CN): δ 51.92, 52.04, 54.43, 55.03, 55.64, 55.75, 63.71, 63.84, 64.32, 64.43, 70.90, 70.96, 72.30, 72.43, 72.62, 72.69, 73.10, 73.39, 73.68, 73.74, 74.25, 75.80. No analysis; decomposes explosively upon heating.

4.6. (3) · 4HClO$_4$

To a stirred solution of **3** (100 mg,) in 10 ml of acetonitrile and 10 ml of water was added dilute $HClO_4$ up to pH < 3. The volume of the solution was reduced by 50% in vacuo whereupon the product precipitates. The tetra-protonated ferrocene cryptand was filtered off and washed with water repeatedly. The yellow product was dried in vacuo for 6 h and recrystallized from CH_3CN–Et_2O (yield, 114 mg (81%)).

^{1}H NMR (CD_3CN) broad lines: δ 3.3 (CH_2), 3.4 (CH_2), 3.61 (CH_2), 3.75 (CH_2), 4.50, 4.52, 4.6 (FcH), 6.8 (NH). ^{13}C NMR (CD_3CN) broad lines: δ 53.32, 55.78, 64.49, 71.03, 72.39, 74.10, 74.98. No analysis; decomposes explosively upon heating.

5. X-ray crystal structure determinations [21]

X-ray data were collected on an Enraf–Nonius CAD4 diffractometer using a graphite monochromator and Mo Kα radiation. An empirical absorption correction (ψ scans) was applied in all cases. Structure solution and refinement was carried out using SHELXS-86 and SHELXL-93 [22].

5.1. (2) · 2 Na(p-tosylate)

The structure was solved using direct methods and refined by the full-matrix least-squares method against F^2. Anisotropic thermal parameters were used for all non-hydrogen atoms except two oxygen atoms O(12) and O(132) in the disordered SO_3 group for which anisotropic refinement proved unstable; for hydrogen atoms the riding model was employed. Single crystals were grown by slowly allowing ether to diffuse into a methanol solution.

5.2. (3) · (RbI)$_2$

The structure was solved using standard Patterson and Fourier methods and refined by the full-matrix least-squares method against F^2. Anisotropic thermal

parameters were used for all non-hydrogen atoms; for hydrogen atoms the riding model was employed. The asymmetric unit contains two disordered $CHCl_3$ molecules on partially occupied positions (site occupancy factor, 0.6 and 0.4). Single crystals were grown from CH_3CN–$CHCl_3$.

5.3. (4) · $Ca(ClO_4)_2 \cdot H_2O$

The structure was solved using direct methods and refined by the full-matrix least-squares method against F^2. Anisotropic thermal parameters were used for all non-hydrogen atoms; for hydrogen atoms the riding model was employed. The perchlorate group is disordered. Single crystals of $4 \cdot Ca(ClO_4)_2 \cdot H_2O$ were grown by allowing ether to diffuse into an acetonitrile solution.

5.4. (4) · $Ba(ClO_4)_2 \cdot H_2O$

The structure was solved using standard Patterson and Fourier methods and refined by the full-matrix least-squares method against F^2. Anisotropic thermal parameters were used for all non-hydrogen atoms; for hydrogen atoms the riding model was employed. Single crystals of $4 \cdot Ba(ClO_4)_2 \cdot H_2O$ were grown by allowing ether to diffuse into an acetonitrile solution. The asymmetric unit contains one molecule of CH_3CN.

5.5. Definition of R values

$R_1 = \Sigma \mid F_o - F_c \mid / \Sigma \ (F_o)$; $wR_2 = [\Sigma[w(F_o^2 - F_c^2)^2] / \mid w(F_o^2)^2]^{1/2}$; goodness of fit $= [\Sigma w(F_o^2 - F_c^2)^2]/(n-p)]^{1/2}$.

Acknowledgment

This work was supported through the Graduiertenkolleg "Ungepaarte Elektronen in Chemie, Physik und Biologie". We wish to thank M. Ruf and H.G. Schmidt for the collection of the X-ray data and Professor H. Vahrenkamp for his support.

References and notes

[1] (a) P.D. Beer, *Adv. Inorg. Chem., 39* (1992) 79; (b) P.D. Beer, *Chem. Soc. Rev., 18* (1989) 409; (c) P.D. Beer, J.P. Danks, D. Hesek and J.F. McAleer, *J. Chem. Soc., Chem. Commun.* (1993) 1735; (d) P.D. Beer, Z. Chen, M.G.B. Drew, J. Kingston, M. Odgen and P. Spencer, *J. Chem. Soc., Chem. Commun.*, (1993) 1046.

[2] (a) M. Delgado, R.E. Wolf, J.R. Hartman, G. McCafferty, R. Yagbasan, S.C. Rawle, D.J. Watkin and S.R. Cooper, *J. Am. Chem. Soc., 114* (1992) 8983; (b) E. Fu, M.L.H. Green, V.J. Lowe, S.R. Marder, G.C. Saunders and M. Tuddenham, *J. Organomet. Chem., 355* (1988) 205; (c) C.D. Hall, J.H.R. Tucker, S.Y.F. Chu, A.W. Parkins and S.C. Nyborg, *J. Chem. Soc., Chem. Commun.*, (1993) 1505; (d) C.D. Hall, I.P. Danks, S.C. Nyborg, A.W. Parkins and N.W. Sharpe, *Organometallics, 9* (1990) 1602; (e) A.R. Ramesha and S. Chandrasekaran, *J. Org. Chem. 59* (1994) 1354; (f) L.F. Joulie, E. Schatz, M.D. Ward, F. Weber and L.J. Yellowlees, *J. Chem. Soc., Chem. Commun.*, (1994) 799.

[3] J.C. Medina, T.T. Goodnow, M.T. Rojas, J.L. Atwood, B.C. Lynn, A.E. Kaifer and G.W. Gokel, *J. Am. Chem. Soc., 114* (1992) 10583.

[4] F.C.J.M. van Veggel, W. Verboom and D.N. Reinhoudt, *Chem. Rev. 94* (1994) 279.

[5] H. Plenio, H. El-Desoky and J. Heinze, *Chem. Ber. 126* (1993) 2403.

[6] H. Plenio, J. Yang, R. Diodone and J. Heinze, *Inorg. Chem. 33* (1994) 4098.

[7] (a) P.D. Beer, D. Hesek, J. Hodacova and S.E. Stokes, *J. Chem. Soc., Chem. Commun.*, (1992) 270; (b) P.D. Beer, C.A.P. Dickson, N. Fletcher, A.J. Goulden, A. Grieve, J. Hodacova and T. Wear, *J. Chem. Soc., Chem. Commun.*, (1993) 828; (c) P.D. Beer, C. Hazlewood, D. Hesek, J. Hodacova and S.E. Stokes, *J. Chem. Soc., Chem. Commun.*, (1993) 1327; (d) P.D. Beer, Z. Chen, A.J. Goulden, A. Graydon, S.E. Stokes and T. Wear, *J. Chem. Soc., Chem. Commun.*, (1993) 1834.

[8] (a) F.P. Schmidtchen, *Nachr. Chem. Tech. Lab., 26* (1988) 8; (b) F.P. Schmidtchen, A. Gleich and A. Schummer, *Pure Appl. Chem., 61* (1989) 1535.

[9] (a) S. Valiyaveetil, J.F.J. Engbersen, W. Verboom and D.N. Reinhoudt, *Angew. Chem., 105* (1993) 942; *Angew. Chem., Int. Edn. Engl. 32* (1993) 900; (b) D.M. Rudkevich, W. Verboom, Z. Brzoka, M.J. Palys, W.P.R.V. Stauthammer, G.J. van Hummel, S.M. Franken, S. Harkema, J.F.J. Engbersen and D.N. Reinhoudt, *J. Am. Chem. Soc., 116* (1994) 4341.

[10] H. An, J.S. Bradshaw and R.M. Izatt, *Chem. Rev. 92* (1992) 543, and references cited therein.

[11] M. Dobler and R.P. Phizackerley, *Acta Crystallogr., Sect. B, 30* (1974) 2746.

[12] M.C. Grossel, M.R. Goldspink, J.P. Knychala, A.R. Cheetham and J.A. Hriljac, *J. Organomet. Chem., 352* (1988) C13.

[13] R.J. Havighurst, E. Mack and F.C. Blake, *J. Am. Chem. Soc. 46* (1924) 2368.

[14] B.P. Hay and J.R. Rustad, *J. Am. Chem. Soc., 116* (1994) 6316.

[15] A.V. Bajaj and N.S. Poonia, *Coord. Chem. Rev. 87* (1988) 55.

[16] B. Metz, D. Moras and R. Weiss, *Acta Crystallogr. Sect. B, 29* (1973) 1377.

[17] R. Hilgenfeld and W. Saenger, in F. Vögtle and E. Weber (eds.), *Host Guest Complex Chemistry — Macrocycles*, Springer, Berlin, 1985.

[18] R.D. Shannon, *Acta Crystallogr. Sect. A, 32* (1976) 751.

[19] (a) S. Akabori, Y. Habata, Y. Sakamoto, M. Sato and S. Ebine, *Bull. Chem. Soc. Jpn. 56* (1983) 537; (b) D. Seyferth, B.W. Hames, T.G. Rucker, M. Cowie and S.D. Raymond, *Organometallics, 2* (1983) 472; (c) M. Cowie and R.S. Dickson, *J. Organomet. Chem., 326* (1987) 269.

[20] V.P. Tverdokhlebov, I.V. Tselinskii, B.V. Gidaspov and G.Y. Chikisheva, *J. Org. Chem. (USSR), 12* (1976) 2268.

[21] Full details of the crystal structure investigations are available on request from the Fachinformationszentrum Chemie, Gesellschaft für wissenschaftlich-technische Information mbH, D-76344 Eggenstein-Leopoldshafen on quoting, together with the names of the authors and the journal citation, the following depository numbers: **2** · 2Na(*p*-tosylate), CSD-400751; **3** · $(RbI)_2$CSD-401116; **4** · $Ca(ClO_4)_2H_2O$, CSD-401117; **4** · $Ba(ClO_4)_2 \cdot H_2O$, CSD-401146.

[22] G.M. Sheldrick, SHELXS-86, University of Göttingen, Göttingen 1986; SHELX-93, University of Göttingen, Göttingen, 1993.